

# Application to Quantify Fetal Lung Branching on Rat Explants

Pedro L. Rodrigues<sup>1,2</sup>, Sara Granja<sup>2</sup>, António Moreira<sup>1,2</sup>, Nuno Rodrigues<sup>3,4</sup> and João L. Vilaça<sup>1,3</sup>

<sup>1</sup>Algoritmi Center, School of Engineering, University of Minho, Guimarães, Portugal

<sup>2</sup>ICVS/3B's, PT Government Associate Laboratory, Braga/Guimarães, Portugal

<sup>3</sup>DIGARC, Polytechnic Institute of Cávado and Ave, Barcelos, Portugal

<sup>4</sup>HASLab/INESC TEC, University of Minho, Braga, Portugal

**Keywords:** Branching Morphogenesis, Lung Development, Image Segmentation, Region-based Algorithms.

**Abstract:** Recently, regulating mechanisms of branching morphogenesis of fetal lung rat explants have been an essential tool for molecular research. The development of accurate and reliable segmentation techniques may be essential to improve research outcomes. This work presents an image processing method to measure the perimeter and area of lung branches on fetal rat explants. The algorithm starts by reducing the noise corrupting the image with a pre-processing stage. The outcome is input to a watershed operation that automatically segments the image into primitive regions. Then, an image pixel is selected within the lung explant epithelial, allowing a region growing between neighbouring watershed regions. This growing process is controlled by a statistical distribution of each region. When compared with manual segmentation, the results show the same tendency for lung development. High similarities were harder to obtain in the last two days of culture, due to the increased number of peripheral airway buds and complexity of lung architecture. However, using semiautomatic measurements, the standard deviation was lower and the results between independent researchers were more coherent.

## 1 INTRODUCTION

Branching morphogenesis is fundamental to the growth and development of several organs such as lung, pancreas, salivary gland, mammary gland, and kidney and prostate. During the last decades, analysis of lung branching morphogenesis of fetal rat explants grown *in vitro* has been an essential tool to the research of the underlying molecular and cellular development mechanisms (Muratore et al., 2009); (Nogueira-Silva et al., 2008). Therefore, this methodology has been widely used in many research centres due to its stability and versatility.

The analysis of branching morphogenesis involves monitoring lung development in explants culture, using images acquired at 24-hours intervals by a stereo microscope during a 5 day period. A morphometric analysis is usually done to study the differentiation and growth of lung explants structure. It quantifies several parameters, such as the inner and outer epithelial perimeter and area and the determination of the number of peripheral airway buds (Nogueira-Silva et al., 2008).

Currently, this analysis is obtained by manual delineation using generic 2D curves software, which

leads to a time-consuming, dependent on user expertise and error-prone procedure. Consequently, this process often results in inaccurate measurements and forbids the comparison among different researchers results (Muehlethaler et al., 2008).

Several image processing strategies have been proposed in the literature to quantify, classify and segment cellular regions from different image sources (Yu and Tan, 2009); (Farjam et al., 2007). In addition, several authors proposed watershed based algorithms to microscope image processing due to its ability to produce closed cell contours (Debeir et al., 2008); (Fan et al., 2008); (Mouelhi et al., 2011).

To best of our knowledge the previous techniques were never applied to this issue. This work presents an image processing application that allows a semiautomatic determination of inner and outer perimeter of lung braches of rat explants cultures.

## 2 METHODS

All methods described below were implemented under C++ and VTK (*Visualization ToolKit*).

## 2.1 Pre-processing Stage

The aims of this stage are the reduction of the noise that corrupts the image, while maintaining and enhancing the relevant object boundaries and selecting a ROI for further processment.

All lung explant images were acquired with an Olympus SZX16 stereo microscope in RGB format. These images were firstly converted to grayscale values by averaging and normalizing the 3 RGB components. Then, the grayscale image was input to an anisotropic diffusion algorithm (implemented as in (Black et al., 1998)). This algorithm depends on three parameters, namely the number of iterations ( $it = 80$ ), edge parameter ( $\sigma=4.5$ ) and a diffusivity function (Tukey's biweight as edge-stopping diffusivity function  $g(x,\sigma)$ , Equation 1) (values were experimentally calculated).

$$g(x, \sigma) = \begin{cases} \frac{1}{2} \left[ 1 - \left( \frac{x}{\sigma} \right)^2 \right]^2 & |x| \leq \sigma \\ 0 & \text{otherwise} \end{cases} \quad (1)$$

The anisotropic diffusion algorithm worked as a Gaussian filter for noise reduction, but with perseverance of sharper boundaries and image contours, producing uniformity in the output image intensity.

Finally, the ROI was selected by removing the existing noise around the lung explant, by cropping its region using a labelling and thresholding algorithm.

## 2.2 Image Partitioning

Since epithelial boundaries of lung explants are often characterized by a significant change in image intensity, an image partitioning yielding meaningful regions is obtained by detecting all the image edges.

Watershed regions were labelled by a starting point and follow the flow line, whose direction was the gradient of intensity, to a local maximum (uphill direction) or minimum (downhill direction). Both directions were implemented, but only the downhill direction was used due to its better performance in the inner lung explants segmentation.

In the end, the whole image is segmented into primitive regions where the boundaries of the watersheds regions coincide with the ridges of the gradient magnitude surface.

The results of the watershed algorithm are oversegmented images as illustrated in Figure 1 (A) and (B).

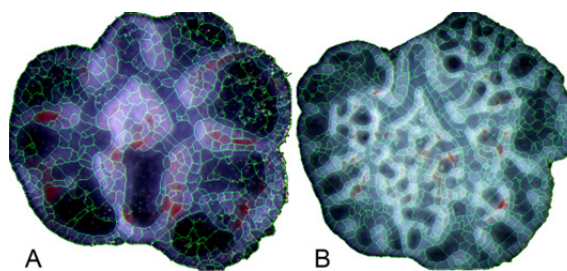


Figure 1: Result of the watershed partitioning in rat lung explants.

## 2.3 Merging Procedure and Inner Lung Explants Quantification

Although the probability that watershed region boundaries correspond to boundaries of important objects increases with oversegmentation, it can also create many insignificant boundaries. This stage describes how one dealt with this problem and the inner lung explants, perimeter and area, were segmented.

Briefly, this procedure consists on the identification of regions edges and its connections with similar intensities, ignoring all others regions with wide mean intensities variations. It assumes that:

1. All pixels within the same region are homogeneous;
2. Regions within lung explant epithelial have homogeneous intensity variations;
3. Regions within lung explant epithelial are considerably different from other outside neighbouring regions;

After establishing the image segmentation through the application of the watershed algorithm, this merging procedure performs feature identification in each region, by identifying the: centroid; mean intensity distribution (MID); minimum and maximum values; region edges; edges region neighbours and the intensity entropy of each region.

Subsequently, the following processing was considered to produce the final merged and segmented result:

The user selects one watershed region within the lung explant epithelial – selected region (SR in red, Figure 2 (A) and (C));

The boundary information of the SR was determined in order to found common intersection edges ( $IE_i$  with  $i = 1, 2, \dots, n$ , Figure 2 - C) between neighbourhood regions  $SRNH$ ;

The MID of each new region ( $MID_{SRNH}$ ) was compared to the MID of the SR ( $MID_{SR}$ ). If  $MID_{SRNH}$  lays between  $MID_{SR} \pm 10\%$ , then the

$IE_i$  (with  $i = 1, 2, \dots, n$ ) is removed and the two regions are merged; The 10% value was experimentally calculated by manually evaluating the mean intensity of the epithelial regions;

If the entropy value of the newly merged region is not within an interval determined by a 90% confidence level, which takes into account the pixel intensity of the two previous regions, these regions should not have been merged; therefore they are unmerged and step 2 is repeated in the opposite direction;

After the merging procedure, the  $SR_{NH}$  with the highest MID similarity value becomes the new SR and step 2 and 4 are repeated (Figure 2 (B) and (D)). This algorithm ends when no  $IE_i$  between similar MID and entropy neighbourhood is found.

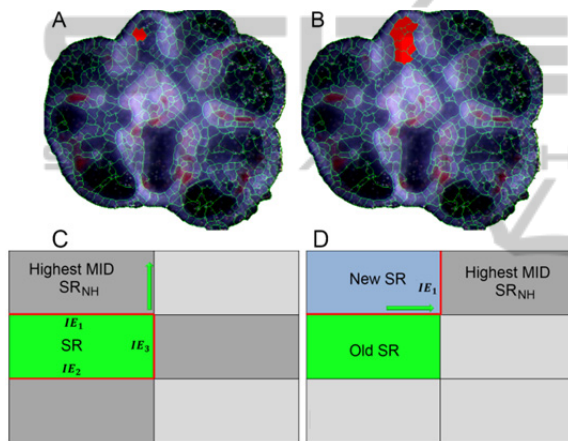


Figure 2: Merging procedure overview.

## 2.4 Outer Lung Explants

Outcome of stage 2.1 was also input to a threshold algorithm in order to determine the outer lung explant area and perimeter, by simply counting the pixels around the object and within it.

## 3 RESULTS

The suitability and validation of the algorithm was conducted on stereo microscope images (Olympus SZX16) acquired at the Life and Health Sciences Research Institute (ICVS) of School of Health Sciences, University of Minho -Portugal. These tests were performed in 50 images, corresponding to images of 10 sets of lung explants on each day of culture. All images were previously segmented by three experienced researchers and this manual segmentation was used as reference for the

evaluation of the algorithm (some results in Fig. 3). Each user manually segmented the same image two times, and the mean and standard deviation of the inner epithelial perimeter for all sets is shown in Table 1.

Table 1: Inner epithelial perimeter results obtained by three different users and by the semiautomatic algorithm.

Culture Day	User 1	User 2	User 3	Interactive Method
1	655 ± 51	645 ± 45	630 ± 42	703 ± 5
2	841 ± 63	850 ± 55	830 ± 70	954 ± 12
3	1565 ± 196	1500 ± 184	1586 ± 177	1752 ± 53
4	2202 ± 313	2380 ± 419	2331 ± 450	2592 ± 56
5	2482 ± 298	2614 ± 506	2800 ± 357	2887 ± 78

Table 2: Summary of the DSC values (%) for each culture day.

Culture Day:	1	2	2	4	5
DSC (%)	92.85 ±3.87	91.54 ±6.12	90.87 ±6.88	88.80 ±9.96	86.72 ±11.75

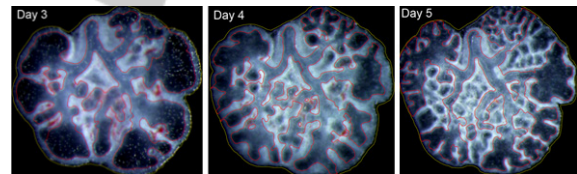


Figure 3: Branching morphogenesis in rat lung explants culture system at each time point. The lines represents the segmentation results of the inner (red) and outer (yellow) epithelial perimeter obtained by the automatic algorithm.

The interactive results were also overlapped with the manual results and its quality and performance were evaluated using the Dice Similarity Coefficient (DSC). The mean DSC, of the interactive method with all the users, from the different days is shown in Table 2, indicating a successful segmentation ( $DSC > 0.85$ ).

## 4 DISCUSSION

An application for image segmentation was developed, providing assistance to the researcher and enabling fast morphometric analysis of lung explants. The total number of decisions to quantify

morphometric analysis was drastically reduced, since the user only has to select one single watershed region.

Generally, best results were obtained in the first two days of culture with lesser standard deviations. High similarities between manual and semiautomatic procedure were harder to get in the last two days of culture, due to the increased number of peripheral airway buds and complexity of lung architecture. The standard deviation of the interactive method was null after all researchers selected the same start region to begin the merging process.

The segmentation rate depended on the number of regions needed to be merged to select the entire region lung epithelial. However, in all cases the interactive segmentation time was less than the manual one ( $34\pm 7\%$  of the manual time).

The merging procedure was essential to achieve a good segmentation, since a lot of regions were firstly created by a watershed algorithm.

Sometimes, the presented method produced undermerged regions due to ambiguity and lack of definition of the inner lung explants contours. These cases increase the probability of merging dissimilar regions and incoherence between boundaries of some watershed regions and boundaries of lung explants inner contours.

## 5 CONCLUSIONS

Regulating mechanisms of branching morphogenesis of fetal lung rat explants have been an essential tool for molecular research. The application of this work provides a technique for lung rat explants segmentation and analysis by selecting only one watershed region belonging to the inner lung epithelial. The total number of decisions, time-consumption and user dependence were significantly decreased.

Further work is needed regarding the merging procedure and the development of image enhancement techniques to improve inner lung epithelial contrast, mainly in the last days of culture, in order to decrease the standard deviation of results and increase its reliability. Moreover, a new algorithm must be developed for counting the number of peripheral airway buds of lung explants.

## ACKNOWLEDGEMENTS

The authors acknowledge to Foundation for Science

and Technology (FCT) - Portugal for the fellowships with the references: SFRH/BD/74276/2010, SFRH/BD/68270/2010, SFRH/BPD/46851/2008 and SFRH/BD/51062/2010.

## REFERENCES

- Black, M. J., Sapiro, G., Marimont, D. H., Heeger, D., 1998. *Robust anisotropic diffusion*. Ieee T Image Process 7, 421-432.
- Debeir, O., Adanja, I., Warzee, N., Van Ham, P., Decaestecker, C., 2008. *Phase contrast image segmentation by weak watershed transform assembly*. I S Biomed Imaging, 724-727.
- Fan, D., Cao, M. Y., Lv, C. Z., 2008. *Wall-adherent cells segmentation based on cross-entropy and watershed transform*. 2008 International Conference on Audio, Language and Image Processing, Vols 1 and 2, Proceedings, 1703-1707.
- Farjam, R., Soltanian-Zadeh, H., Jafari-Khouzani, K., Zoroofi, R.A., 2007. *An image analysis approach for automatic malignancy determination of prostate pathological images*. Cytometry Part B: Clinical Cytometry 72B, 227-240.
- Mouelhi, A., Sayadi, M., Fnaiech, F., 2011. *Automatic segmentation of clustered breast cancer cells using watershed and concave vertex graph*, Communications, Computing and Control Applications (CCCA), 2011 International Conference on, pp. 1-6.
- Muehlethaler V, K. A., Seedorf G, Balasubramaniam V, Abman SH., 2008. *Impaired VEGF and nitric oxide signaling after nitrofen exposure in rat fetal lung explants*. Am J Physiol Lung Cell Mol Physiol. 294, 110-130.
- Muratore CS, L. F., Zhou Y, Harty M, Reichner J, Tracy TF., 2009. *Endotoxin alters early fetal lung morphogenesis*. J Surg Res 155, 225.
- Nogueira-Silva C, M. R., Esteves N, Gonzaga S, Correia-Pinto J., 2008. *Intrinsic catch-up growth of hypoplastic fetal lungs is mediated by interleukin-6*. Pediatr Pulmonol 43, 680-689.
- Yu, J., Tan, J., 2009. *Object density-based image segmentation and its applications in biomedical image analysis*. Computer Methods and Programs in Biomedicine 96, 193-204.